Author's reply – Hannah Davies – Back to the future II: Tidal evolution of four supercontinent scenarios.

Dear Editor,

Myself and my co-authors would like to thank you for your moderation of this manuscript. Through your and the reviewers' comments and guidance, we believe the manuscript is now improved from its original submission. Please find below our response to each reviewer's comments, and the changes we have made to the manuscript as a result of the input of the reviewers.

Response to reviewer 1:

Firstly, all the authors of this manuscript would like to thank Daniel Pastor-Galán for his insightful and constructive comments on the paper.

1. "I feel the discussion is a little limited. It verses mostly about the size (4500 Km) of ocean width".

The 4500 Km ocean width and the equations mentioned in the discussion represent the main conclusions of the paper. We wanted to show that we had experimentally verified the ocean width and depth required for resonance. The discussion has been expanded as a result of this, and other comments by both reviewers.

2. Reviewer 1 mentions that a more synthetic analysis of the tide in oceans with various simplified or facsimile shapes i.e. the Tethys/annular/circular/triangular.

Synthetic modelling of different shaped oceans which close at different angles was tested, and it was deemed too much to present both the synthetic and the future supercontinent model results in one paper. Detailed synthetic modelling (covering the ocean and continent arrangements mentioned by the reviewer in their first, second and third comments) is currently ongoing with the aim of producing enough results to publish in a separate paper.

3. "I am convinced that tidal cycles are intrinsically linked to the Wilson cycle in 4D: when, how quick and where oceans open control the tides. Do you really think there is a supercontinent-supertide connection?"

We would still like to argue for a supercontinent-super-tide connection because even though the tide does change predominantly with the progression of the Wilson cycle, i.e. after the ocean has opened sufficiently it will pass through at least one tidal resonance, there is still a long term trend occurring. In all scenarios we see a trend of stronger average tides during the dispersed continent phase of a supercontinent cycle, and weaker average tides during the gathered phase of the supercontinent cycle. We clarified this idea further in the discussion section of the manuscript.

4. "Line 10:"Ma""

We agree that Myr is a more widespread unit and have therefore changed "Ma" to Myr" throughout the manuscript.

5. "Line 29: I think Trond's and my paper suggest that it might be. Other authors are more convinced about it, but Perhaps Trond and I are among the people that think that maybe it is linked to everything and maybe it is not."

Acknowledged, updated manuscript to include ongoing discussion

6. "Lines 129-130: Is this error +/-12. Is it just 12 cm over or under the maximum tide? Isa +/-6? Please specify. In general, I think the way the uncertainty is treated over the paper is superficial."

Root mean square error represents the standard deviation of the error, so 12 is the amount the model results deviate from the observed result of the M2 tide. This value can apply as positive or negative, either side of the "line of best fit of the data" (which in this case is measured "real world" tidal values). We clarified the whole section presenting error and uncertainty in the manuscript.

7. "Lines 236-237: This is particularly interesting. Considering the particularities of supertidal periods, you should try getting a rough estimate (Fermi problem style) of how often such things had happened through Earth history... And check if that fit with our knowledge of global tectonics and moon formation etc..."

Myself and my co-authors were very intrigued by this comment and have since added a fermi equation to the manuscript in the discussion. We have added a table 2 which summarises the total time each scenario was in a super-tidal state. We also removed two paragraphs in the discussion which were deemed less pertinent now this fermi style problem has been discussed. As a result, we believe the discussion is now more directed at discussing the results.

Response to reviewer 2:

We would like to thank anonymous reviewer 2 for their helpful and constructive comments on the paper.

1. "Could the authors provide some comment as to the choice of modelling only the M2 constituent (and not including K1 for example), and on why they retain the Earth-Moon orbit configuration (specifically the 12.42 hr period forcing) throughout the future simulations? Are there projections as to how this may to change within 250Ma that may be referenced? It will impact the age/size at which future ocean basin configurations form tidal resonance. This prompts a thought on the validity of the extrapolation of particular values (particularly the buoyancy frequency and ocean volume) from present day climatology for the calculation of tidal dissipation/amplitude in the future scenarios. Can the authors address these simplifications to their simulations?"

Modelling was carried out initially with both the M2 and the K1 constituents however the volume of data quickly became too much to present concisely in one paper. Furthermore, not only did the results for the K1 constituent corroborate the hypothesis of resonance - albeit at different wavelengths and ocean sizes - the tidal energy dissipated as a result of the K1 constituent was an order of magnitude lower than the M2 making it less impactful to the overall tidal environment.

With regards to the change in tidal, oceanographic, and orbital parameters over the period modelled (250 Myr) we have since added a paragraph to the results section of the manuscript presenting the change in tidal period and lunar forcing over time.

2. "Could the authors state clearly if equilibrium forcing is used at the pole boundaries in this study (as done in Green et al. 2018) or if vertical walls were used – the reading from Line 117 is slightly ambiguous. Since this study provides higher temporal resolution for future continent configurations from Green et al. 2018, does the equilibrium forcing (or vertical wall) at the boundary interfere with any potential tidal resonance in basins/enclosures present in this study but not present in the scenarios Green et al. 2018 considered? It is difficult to tell from the map projection used for the figures in the supplement."

Equilibrium forcing at the poles was not used (as done in Green et al., 2018), vertical walls at the poles were used. The introduction of an open boundary with an equilibrium tide as forcing does not change the results. Furthermore the inclusion of walls does interfere with resonance; however, it is only observed once to minimal effect, (during the Aurica scenario) nonetheless, is mentioned in the discussion. The methods mentioned in line 117 have been clarified in the revised manuscript.

3. "Regarding the 4 km deep ocean calculation at Line 209: Does the average depth of any ocean basin change significantly to retain ocean volume between the four future scenarios (e.g. due to differing continent

polygon overlap and/or destruction of shelves)? How applicable is this calculation of when resonance occurs for the multiple different basin shapes shown in the different scenarios?”

Changing ocean depth does influence the resonant width of the ocean however the deviation from 4 Km in the models to retain ocean volume is not significant to change ocean resonance by a large amount. We have updated the manuscript to show that the resonant width scales with the square root of the depth so to change the resonance of the ocean, the depth must change by a factor of four.

4. “The paper professes to support a link between the super-tidal and super-continent cycles. Since each continent cycle may be comprised of one or multiple Wilson cycles (to which a super-tidal cycle seems more intrinsically linked to), is there not a lack of a well-defined relationship between the period of each?

The Supercontinent cycle, Wilson cycle, and Super-tidal cycle are secularly linked. We have clarified the link between the three cycles and their relationship with regards to the super-tidal cycle in the manuscript.

All technical corrections suggested by reviewer 2 have been made in the manuscript:

Technical corrections: line 11 – remove comma after “planet”

Done.

line 11 – Perhaps “...oceans *can* move...”

Clarified this sentence and improved its structure.

line 47 – “at best” is strange wording, perhaps “at a minimum of”

Agreed, changed in manuscript.

lines 75-80 – various subscripts are printed as normal sized text

Subscripts corrected.

line 129 – I assume “The results” refer to amplitudes. Could this be made clearer what is being compared to TPXO9.

This whole section has been revised as a result of both reviewer comments

line 152 – is PD defined in the text before its first use here?

PD now defined as "Present-day" in first use.

line 246 – “...which, when combined, produce...”

Improved sentence structure.

Back to the Future II: Tidal evolution of four supercontinent scenarios

Hannah S. Davies[1,2], J.A. Mattias Green[3], Joao C. Duarte[1,2,4]

[1]Instituto Dom Luiz (IDL), Faculdade de Ciências, Universidade de Lisboa, Campo Grande, 1749-016, Lisboa, Portugal
[2]Departamento de Geologia, Faculdade de Ciências, Universidade de Lisboa, Campo Grande, 1749-016, Lisboa, Portugal,
[3]School of Ocean Sciences, Bangor University, Askew St, Menai Bridge LL59 5AB, UK
[4]School of Earth, Atmosphere and Environment, Monash University, Melbourne, VIC 3800, Victoria, Australia

Correspondence to: Hannah S. Davies (hdavies@fc.ul.pt)

Abstract. The Earth is currently 180 ~~Ma~~Myr into a supercontinent cycle that began with the breakup of Pangea, and will end in around 200 – 250 ~~Ma~~Myr (Million years~~ega annum~~) in the future, as the next supercontinent forms. As the continents move around the planet~~,~~ they change the geometry of ocean basins, and thereby modify their resonant properties. In doing so oceans move through tidal resonance, causing the global tides to be profoundly affected. Here, we use a dedicated and established global tidal model to simulate the evolution of tides during four future supercontinent scenarios. We show that the number of tidal resonances on Earth vary between 1 and 5 in a supercontinent cycle, and that they last for no longer than 20 ~~Ma~~Myr. They occur in opening basins after about 140 – 180 ~~Ma~~Myr, an age equivalent to the Present-Day Atlantic Ocean, which is near resonance for the dominating semi-diurnal tide. They also occur when an ocean basin is closing, highlighting that in its lifetime, a large ocean basin – its history described by the Wilson cycle – may go through two resonances: one when opening and one when closing. The results further support the existence of a super-tidal cycle associated with the supercontinent cycle, and gives a deep-time proxy for global tidal energetics.

1 Introduction

The continents have coalesced into supercontinents and then dispersed several times in Earth's history in a process known as the supercontinent cycle (Nance et al., 1988). While the cycle has an irregular period (Bradley, 2011), the breakup and reformation typically occurs over 500 – 600 ~~Ma~~Myr (Nance et al., 2013; Davies et al., 2018; Yoshida and Santosh, 2017; 2018). Pangea was the latest supercontinent to exist on Earth, forming ~300 ~~Ma~~Myr ago, and breaking up around 180 ~~Ma~~Myr ago, thus initiating the current supercontinent cycle (Scotese, 1991; Golonka, 2007). Another supercontinent should therefore form within the next 200 – 300 ~~Ma~~Myr (e.g., Scotese 2003; Yoshida, 2016; Yoshida and Santosh, 2011 and 2017; Duarte et al., 2018; Davies et al., 2018).

The supercontinent cycle is believed to be an effect of plate tectonics and mantle convection (Torsvik, 2010 and 2016; Pastor-Galan, 2018), and the breakup and accretion of supercontinents are a consequence of the opening and closing of ocean basins (Wilson, 1966; Conrad and Lithgow-Bertelloni, 2002). The life cycle of each ocean basin is known as the Wilson cycle. A supercontinent cycle may comprise more than one Wilson cycle since several oceans may open and close between the breakup and reformation of a supercontinent (e.g., Hatton, 1997; Murphy and Nance, 2003; Burke, 2011; Duarte et al., 2018; Davies et al., 2018).

As ocean basins evolve during the progression of the Wilson cycle (and associated supercontinent cycle), the energetics of the tides within the basins also change (Kagan, 1997; Green et al., 2017). Green et al. (2017; 2018) simulated the evolution of tides from the breakup of Pangea until the formation of a future supercontinent, thus spanning a whole supercontinent cycle, and found a link between Wilson cycles and tides. They also found that the unusually large present-day tides in the Atlantic, generated because of the near-resonant state of the basin (Platzman~~n~~, 1975; Egbert et al., 2004; Green, 2010; Arbic and Garett, 2010), have only been present for the past 1 ~~Ma~~Myr. However, because the Atlantic is still spreading apart, it will eventually become too wide to sustain resonant tides in the near (geological) future. But when exactly will this happen, and is it possible that while the continents diverge and converge, other basins will reach the right size to become resonant?

The initial simulation of deep-time future tides by Green et al. (2018)~~, conducted by Green et al., (2018) using~~ used a scenario of the Earth's tectonic future presented by Duarte et al. (2018), and strengthened the proof-of-concept for the existence of a super-tidal cycle associated with the supercontinent cycle. Their simulations were done using 50-100 Myr intervals between simulations. They acknowledged that this was not enough to resolve details of the future tidal maxima, including their duration. ~~Their simulations were done using~~ ~~, at best, 50 Ma intervals between most of the time slices, which Green et al. (2018)~~the authors ~~suggested was not enough to resolve details of the future tidal maxima, principally, their duration.~~

In this work, we therefore revisit the future evolution of Earth's tides by simulating the tide at 20 ~~Ma~~Myr intervals during the four different tectonic modes of supercontinent formation summarised by Davies et al. (2018): Pangea Ultima (based on Scotese, 2003), Novopangea (Nield, 2007), Aurica (Duarte et al., 2018) and Amasia (based on Mitchell et al., 2012). Pangea Ultima is a scenario governed by the closing of the Atlantic – an interior ocean – leading to the reformation of a distorted Pangea (Murphy and Nance 2003 and 2008 call this "closure through introversion"). Novopangea, in contrast, is dominated by the closing of the Pacific Ocean – an exterior ocean – and the formation of a new supercontinent at the antipodes of Pangea (this is closure through extroversion; Murphy and Nance 2003). Aurica is a scenario in which the Atlantic and the Pacific close simultaneously and a new ocean opens across Siberia, Mongolia, and India, bisecting Asia (a combination scenario in which two oceans close, one by introversion and another by extroversion; Murphy and Nance 2005; Duarte et al., 2018). Finally, in the Amasia scenario, the continents gather at the North Pole, 90º away from Pangea (this is known as orthoversion; Mitchell et al., 2012). Every scenario has the potential to develop different tidal resonances in different ocean basins at different stages in each ocean's evolution. We focus here on identifying the timing of the occurrence of resonant basins, and on mapping the large-scale evolution of tidal amplitudes and tidal energy dissipation rates in each of the investigated scenarios. We were particularly interested in understanding how common the resonant "super-tidal" states are, for how long they last, and their relationship with the Wilson cycle.

2 Methods

2.1 Tidal modelling

The future tide was simulated using the Oregon State University Tidal Inversion Software, OTIS, which has been extensively used to simulate global-scale tides of the past, present, and future (Egbert et al., 2004; Green, 2010; Green and Huber, 2013, Wilmes and Green, 2014; Green et al., 2017; 2018). OTIS was benchmarked against other software that simulate global tides and it was shown to perform well (Stammer et al., 2014). It provides a solution to the linearized shallow water equations (Egbert et al., 2004):

$$\frac{\partial \boldsymbol{U}}{\partial t} + f \times \boldsymbol{U} = gh\nabla(\eta - \eta_{SAL} - \eta_{EQ}) - \mathbf{F} \quad (1)$$

$$\frac{\partial \eta}{\partial t} - \nabla \cdot \boldsymbol{U} = 0 \quad (2)$$

Here, **U** is the tidal volume transport vector defined as **u***h*, where **u** is the horizontal velocity vector and h the water depth, *f* is the Coriolis parameter, *g* the acceleration due to gravity, η the sea surface elevation, η_{SAL} the self-attraction and loading elevation, η_{EQ} the elevation of the equilibrium tide, and **F** the energy dissipation term. The latter is defined as **F** = **F**b + **F**w, where **F**b = Cd**u**|**u**| parameterises energy due to bed friction using a drag coefficient, Cd=0.003, and **F**w =C**U** represents losses due to tidal conversion. The conversion coefficient, C, is based on Zaron and Egbert (2006) and modified by Green and Huber (2013), computed from:

$$C(x,y) = \gamma \frac{N_H \bar{N}}{8\pi\omega} (\nabla H)^2 \quad (3)$$

in Eq. (3) γ = 50 is a dimensionless scaling factor accounting for unresolved bathymetric roughness, N_H is the buoyancy frequency (*N*) at seabed, $\bar{N}$ is the vertically averaged buoyancy frequency, and ω is the frequency of the M_2 tidal constituent, the only constituent analysed here. The buoyancy frequency, *N*, is based on a statistical fit to present day climatology (Zaron and Egbert, 2006), and given by N(x,y) = 0.00524exp(-z/1300), where z is the vertical coordinate counted positive upwards from the sea floor. *N* was kept constant throughout the simulations because there is no quantitative way to estimate buoyancy frequency for the future simulations. We did not change *N* throughout the simulations because the stratification in the future oceans is yet to be quantified.

Each run simulated 14 days, of which 5 days were used for harmonic analysis of the tide. The model output consists of amplitudes and phases of the sea surface elevations and transports, which was used to compute tidal dissipation rates, *D*, as the difference between the time average of the work done by the tide generating force (*W*), and the divergence of the horizontal energy flux (**P**; see Egbert and Ray, 2001, for details):

$$D = W - \nabla \cdot \mathbf{P} \quad (4)$$

where W and P are given by:

$$W = g\rho\mathbf{U} \cdot \nabla(\eta EQ + \eta SAL) \quad (5)$$

$$\mathbf{P} = g\rho\mathbf{U}\eta \quad (6)$$

The orbital configuration of the Earth-Moon system, and thereby the tidal and lunar forcing was not changed during the future simulation. The difference in tidal period (+0.11 hr) and lunar forcing (-3%) that occurs after 250 Myr was applied to a sensitivity simulation which found that the altered parameters do not affect the results sufficiently to warrant changing the values from present-day.

2.2 Mapping of future tectonic scenarios

We coupled the kinematic tectonic maps produced by Davies et al. (2018) with OTIS at incremental steps of 20 Ma Myr by using the tectonic maps as boundary conditions in the tidal model. The maps were produced using GPlates, a software specifically designed for the visualisation and manipulation of tectonic plates and continents (e.g., Qin et al., 2012; Muller et al., 2018). We used GPlates to digitise and animate a high resolution representation of present-day continental shelves and coastline (with no ice cover), created from the NOAA ETOPO1 global relief model of the Earth (see https://data.nodc.noaa.gov/cgi-bin/iso?id=gov.noaa.ngdc.mgg.dem:316# for details). For a matter of simplification, shelf extents are kept for the full duration of the scenarios. The continental polygons do not deform, though some overlap is allowed between their margins, to simulate rudimentary continental collision and shortening. Intracontinental breakup and rifting were introduced in three of the scenarios, allowing new ocean basins to form. No continental shelves were extrapolated along the coastlines of these newly formed basin's margins. For more details on the construction of the tectonic scenarios and the respective maps, see Davies et al. (2018).

The resulting maps were then given an artificial land mask 2° wide on both poles to allow for numerical convergence (simulations with equilibrium tides near the poles in Green et al., 2017; 2018 did not change the results there), and were constrained to a horizontal resolution of ¼°º in both latitude and longitude. They were then assigned a simplified bathymetry; continental shelves were set a depth of 150 m, and mid-ocean ridges were assigned a depth of 1600 m at the crest point and deepening to the abyssal plains within a width of 5°. Subduction trenches were made 5800 m deep., The depth of the abyssal plains in the maps changes dynamically to retain present-day ocean volume throughout the scenarios. This was to allowallows the tidal results of the future simulations to be more comparable to thea present-day simulation, result which was tested against real world tidal observations. with the abyssal plains being set to a depth maintaining present-day ocean volume. The resulting maps were averaged to a horizontal resolution of ¼° in both latitude and longitude.

To test the accuracy of our results, weWe pralso produced and used two present-day bathymetries to test the accuracy of our results. The first – a present-day control - is based on v13 of the Smith and Sandwell bathymetry (Smith and Sandwell, 1997; https://topex.ucsd.edu/marine_topo/). A second map was then produced – the present-day degenerate bathymetry – which included a bathymetry created by using the depth values and the method described for the future slices (see Fig. 1 and corresponding description in section 2.2).

3 Results

The tidal amplitude results for the present-day control simulation (Fig. 1c), when compared to the TPX09 satellite altimetry constrained tidal solution (Egbert and Erofeeva, 2002; http://volkov.oce.orst.edu/tides/tpxo9atlas.html), produced an RMS error of ±12 cm. Comparing the present-day degenerate simulation (Fig. 1d) results to TPXO9, resulted in an RMS error of ±13 cm. This is consistent with previous work (Green et al., 2017; 2018) and gives us a quantifiable error of the model's performance when there is a lack of topographic detail (e.g., as in our future simulations).

The present-day control simulation (Fig. 1e) has a dissipation rate of 3.3 TW, with 0.6 TW dissipating in the deep ocean. This corresponds to 137% of the observed (real) global dissipation rate (2.4 TW for M2, see Egbert et al., 2004), and 92% of the measured deep ocean rates (0.7 TW). The present-day degenerate bathymetry underestimates the globally integrated dissipation by a factor of 0.9, and the deep ocean rates by a factor of ~0.8 (Fig. 1f). Sensitivity simulationstests offor the present-day control simulation with varying bed friction and buoyancy frequency did not produce any significant difference in the result. The future tidal dissipation results (Fig. 3) were therefore normalised against the degenerate present-day value (2.2 TW), to account for the bias due to underrepresented bathymetry caused when using the simplified bathymetry in the future simulations (see Green et al., 2017, for a discussion).

The resulting tidal amplitudes and associated integrated dissipation rates are shown in Figs 2, 4-6 (amplitudes), and Fig. 3 (dissipation). The latter is split into the global total rate, and rates in shallow (depths of < 500m), and deep water (depths of > 500m; Egbert and Ray, 2001), to highlight the mechanisms behind the energy loss. In the following we define a super-tide as occurring when: i) tidal amplitudes in a basin are on average meso-tidal or above, i.e., larger than 2 m, and ii) the globally integrated dissipation is equivalent to or larger than present-day values.

3.1 Pangea Ultima

In the Pangea Ultima scenario, the Atlantic Ocean continues to open for another 100 ~~Ma~~Myr, after which it starts closing, leading to the formation of a slightly distorted new Pangea in 250 ~~Ma~~Myr (Fig. 2 and Video S1 in the Supplementary Material). The continued opening of the Atlantic in the first 60 ~~Ma~~Myr moves the basin out of resonance, causing the M_2 tidal amplitude and dissipation to gradually decrease (Figs. 2 and 3a). During this period, the total global dissipation drops to below 30% of the PD (present-day) rate (note that this is equivalent to 2.2 TW because we compare to the degenerate bathymetry simulation), after which, at 80 ~~Ma~~Myr, it increases rapidly to 120% of PD (Figs. 3a and 2b). This peak at 80 ~~Ma~~Myr is due to a resonance in the Pacific Ocean initiated by the shrinking width of the basin (Fig. 2b). The dissipation then drops again until it recovers and peaks around 120 ~~Ma~~Myr at 130% above PD (Fig. 3a). This second peak is caused by another resonance in the Pacific, combined with a local resonance in the Northwest Atlantic (Fig. 2c). This period also marks the initiation of closure of the Trans-Antarctic ocean, a short-lived ocean which began opening at 40 ~~Ma~~Myr and was microtidal for its entire tenure (Fig. 2a-c). A third peak then occurs at 160 ~~Ma~~Myr, the most energetic period of the simulation, with the tides being 215% more energetic than at present due to both the Atlantic and the Pacific being resonant for M_2 frequencies (Fig. 2d). After this large-scale double resonance, the first described in detail in deep-time simulations, and the most energetic relative dissipation rate encountered, the tidal energy drops, with a small recovery occurring at 220 ~~Ma~~Myr due to a further minor Pacific resonance (Fig. 2e). When Pangea Ultima forms at 250 ~~Ma~~Myr (see Fig. 2f), the global energy dissipation has decreased to 25% of the PD value, or 0.5TW (Fig. 2f).

3.2 Novopangea

In the Novopangea scenario, the Atlantic Ocean continues to open for the remainder of the supercontinent cycle. Consequently, the Pacific closes, leading to the formation of a new supercontinent at the antipodes of Pangea in 200 ~~Ma~~Myr (Fig. 4 and Video S2 in the Supplementary Material). As a result, within the next 20 ~~Ma~~Myr the global M_2 dissipation rates decrease to half of present-day values (see Fig. 3b and 4 for the following discussion). The energy then recovers to PD levels at 40 ~~Ma~~Myr as a result of the Pacific Ocean becoming resonant. From 40 ~~Ma~~Myr to 100 ~~Ma~~Myr, the dissipation rates drop, reaching 15% of the PD value at 100 ~~Ma~~Myr. There is a subsequent recovery to values close to 50% of PD, with a tidal maximum at 160 ~~Ma~~Myr due to local resonance in the newly formed East-African Ocean (Davies et al., 2018). Even though the tidal amplitude in this new ocean reaches meso-tidal levels (i.e., 2-4 m tidal range, Fig. 3b), the increased dissipation in this ocean only increases the global total tidal dissipation to 50% PD (Fig. 4e). Therefore, this ocean cannot be considered super-tidal. The tides then remain at values close to half of present-day, i.e., equal to the long-term mean over the past 250 ~~Ma~~Myr in Green et al. (2017), until the formation of Novopangea at 200 ~~Ma~~Myr. After 100 ~~Ma~~Myr there is a regime shift in the location of the dissipation rates, with a larger fraction than before dissipated in the deep ocean (Fig. 3b).

3.3 Aurica

Aurica is characterized by the simultaneous closing of both the Atlantic and the Pacific Oceans, and the emergence of the new Pan-Asian Ocean. This allows ~~allow~~ Aurica to form via combination in 250 ~~Ma~~Myr (Fig. 5 and Video S3 in the Supplementary Material). In this scenario, the tides remain close to present-day values for the next 20 ~~Ma~~Myr (see Fig. 3c and 5 for the results), after which they drop to 60% of PD at 40 ~~Ma~~Myr, only to rise to 114% of PD values at 60 ~~Ma~~Myr and then to 140% of PD rates at 80 ~~Ma~~Myr. This period hosts a relatively long super-tidal period, lasting at least 40 ~~Ma~~Myr as the Pacific and

Atlantic go in and out of resonances at 60 ~~Ma~~Myr and 80 ~~Ma~~Myr, respectively. The dissipation then drops to 40-50% of PD, with a local peak of 70% of the PD value at 180 ~~Ma~~Myr due to resonance in the Pan-Asian Ocean. This is the same age as the North Atlantic today, which strongly suggests that oceans go through resonance around this age. By the time Aurica forms, at 250 ~~Ma~~Myr, the dissipation is 15% of PD, the lowest of all simulations presented here.

3.4 Amasia

In the Amasia scenario, all the continents except Antarctica move north, closing the Arctic Ocean and forming a supercontinent around the North Pole in 200 ~~Ma~~Myr (Fig. 6 and Video S4 in the Supplementary Material). The results show that the M_2 tidal dissipation drops to 60 % of PD rates within the next 20 ~~Ma~~Myr (Fig. 3d and 6 for continued discussion). This minimum is followed by a consistent increase, reaching 80% of PD rates at 100 ~~Ma~~Myr, and then, after another minimum of 40% of PD rates at 120 ~~Ma~~Myr, tidal dissipation increases until it reaches a maximum of 85% at 160 ~~Ma~~Myr. These two maxima are a consequence of several local resonances in the North Atlantic, North Pacific, and along the coast of South America, and the minimum at 120 ~~Ma~~Myr is a result of the loss of the dissipative Atlantic shelf areas due to continental collision. A major difference between Amasia and the scenarios previously described, is that here we never encounter a full basin-scale resonance. This is because the circumpolar equatorial ocean that forms is too large to host tidal resonances, and the closing Arctic Ocean is too small to ever become resonant. However, the scenario is still rather energetic, with dissipation rates averaging around 70% of PD rates because of several local areas of high tidal amplitudes and corresponding high shelf dissipation rates (Fig. 3d).

4 Discussion

We investigated how the tides may evolve during four probable scenarios of the formation of Earth's future supercontinent. The results show large variations in tidal energetics between the scenarios (see Table 1 and Fig. 3), with the number of tidal maxima ranging from 1 (~~i.e.,~~ at present during the Amasia scenario) to 5 (including today's in the Pangea Ultima scenario) – see Table 1 for a summary. These maxima occur because of tidal resonances in the ocean basins as they open and close. Furthermore, we have shown that an ocean basin becomes resonant for the M_2 tide when it is around 140 – 180 ~~Ma~~ Myr old (as is the PD Atlantic). The reason for this is simple: assuming the net divergence rate of two continents bordering each side of an ocean basin is ~3 cm yr^{-1} (which is close to the average drift rates today), after 140 ~~Ma~~Myr it will be 4500 km wide. Tidal resonance occurs when the basin width is half of the tidal wavelength (Arbic and Garrett, 2010):~~,~~

$$L = c_g T \qquad (7)$$

~~$L = c_g T$~~

~~(Arbic and Garrett, 2010),~~ where the wave speed ~~can be derived~~is given by:

$$c_g = (gh)^{1/2} \qquad (8)$$

~~$c_g = (gh)^{1/2}$~~

~~is the wave speed~~ and T is the tidal period (~~here equal to~~ 12.42 hours). For a 4000 m deep ocean, resonance thus occurs when the ocean is ~~around~~ 4429~~500~~ k~~K~~m wide, i.e. at the age given above. The depth of the simulated oceans changes between the scenarios to preserve ocean volume at that of present day. These changes are too small to affect the resonant scales in the different simulations, especially at the resolution we are using here (1/4° in latitude and longitude). For example, in the Novopangea scenario, which has the shallowest average ocean depth at 3860 m, the resonant basin scale is 4350 km, whereas in the Pangea Ultima scenario, in the present-day the overall deepest at 4395 m, the basin scale would be 4642 km. This ~~This~~

is a key result of this investigation, and again highlights the relationship between the tidal and tectonic evolution of an ocean basin. It also reiterates that ocean basins must open for at least 140 MaMyr to be resonant during their opening at present day drift speeds (e.g., the Pan-Asian ocean)(or drift much faster that at present), e.g. the Pan-Asian ocean. If an ocean opens for less than 140 MaMyr, e.g. the Trans-Antarctic (80 MaMyr of opening) or Arctic ocean (60 MaMyr of opening; Miller et al., 2006), or if they drift slower than 3 cm yr^{-1}, they will not become resonant or even mesotidal. After this 140 MaMyr/4500 kKm age/width threshold has been reached, the ocean may then be resonant again if it closes.

Therefore, if the geometry, and mode of supercontinent formation permits (i.e., multiple Wilson cycles are involved), several oceans may go through multiple resonances – sometimes simultaneously – as they open/close, during a supercontinent cycle. For example, during in the Pangea Ultima scenario, the Atlantic and Pacific are simultaneously resonant at 160 MaMyr (Table 1), and as Aurica forms, the Atlantic is resonant twice (at present, and when closing at 80 MaMyr), the Pacific once (closing) and the Pan-Asian ocean once (after 180 MaMyr, when opening; Table 1 and section 3.3).

The simulations here expand on the work of Green et al., (2018), regarding the tidal evolution of Aurica. They find a more energetic future compared to the present Aurica simulations (e.g., our Fig. 3c): their average tidal dissipation is 84% of the PD value, with a final state at 40% of PD, whereas we find dissipation at 64% of PD on average and 15% of PD at 250 MaMyr. This discrepancy can be explained by two factors present in the work of Green et al. (2018): a lack of temporal resolution, and a systematic northwards displacement in the configuration of the continents, meaning their tidal maxima are exaggerated. Despite these differences, the results are qualitatively similar, and we demonstrate here that under this future scenario the tides will be even less energetic than suggested in Green et al. (2018). This, along with results from tidal modelling of the deep past (Green et al., 2017, 9 in review, Byrne et al., 2019 in review, Green and Hadley-Pryce personal comm. 2019, and this paper, and unpublished results) lends further support to the super-tidal cycle concept, and again shows how strong the current tidal state is.

Present Lunar recession rates also expose the anomalous current tidal state. Retropolating present Lunar recession rates into deep time (~3.8 cm yr^{-1}; Dickey et al., 1994) places lunar formation at 1.5 Ga in Earth History. However, the Moon is geologically aged at 4.5 Ga (Kleine et al., 2005). This disparity in Lunar ages confirms that tidal dissipation rates must have been – except for occasional super-tidal periods – a fraction of the present-day value for most of deep time. The present-day tidal anomaly represents a hurdle for deep time climate models. This can be seen in the Eocene, where the dissipation rates from Green and Huber (2013) solved a decade long problem of reconstructing a model of the Eocene climate which conforms to the paleo-climate record (Huber et al., 2003). They found the global total tidal dissipation at 55 Ma was around 1.44 TW, with 40 % of that being dissipated in the deep Pacific Ocean, a regime significantly different to the present-day, but enough to sustain abyssal mixing that could reduce meridional temperature gradients (Green and Huber 2013).

This study represents one of many tidal modelling projects with OTIS (see Green et al., 2017; 2018, and Davies et al., 2018 for discussions) which combined, produce a suite of sensitivity simulations. Despite the fact that the method of assigning bathymetry was different here, and in other papers, and the values of γ and C_d in Eqs. (1)-(2) were changed, every result shows changes differing by no more than 10-20% of the results presented here. Further sensitivity simulations can be done in the future as our modelling capacity increases, but at this stage, we argue that our results are robust and realistic.

All four scenarios presented have an average tidal dissipation lower than the present-day, and all scenarios, except Amasia, have a series of super-tidal periods analogous to present-day. The results presented here can supplement the fragmented tidal record of the deep past (Kagan and Sundermann, 1996; Green et al., 2017) and allow us to draw more detailed conclusions about the evolution of the tide over geological time, and the link between the tide, the supercontinent cycle, and the Wilson cycle.

Using the data and conclusions above, and several assumptions, wWe have constructedestimated a super-tidal “Fermi problem/Drake equation” for thethe frequency ofnumber tidal maxima that have occurred in the Earth’s history (Nf_{tot}) -and the total time that the Earth was in a super tidal state (T), as follows: period of resonant tidal dissipation (T_{tot}) of Supertidal periods in Earth History:

$$f_{tot}N = N_{sc} \cdot N_{wc} \cdot fN_{wtc} \qquad (9)$$

WhereAnd:

$$T_{tot}T = \frac{f_{tot}N * PT_{tm}}{PT_{pEt}} \qquad (10)$$

N_{sc} represents the Number of supercontinent cycles whichthat have occurred on Earth, including the present one (we assume a minimum of 5 supercontinent cycles or 6; e.g. Davies et al., 2018; and references therein), N_{wc} is the number of Wilson cycles per supercontinent cycle initiated/terminated, and reaching maturitythat have supported a super tide (>140 Myr) per Supercontinent cycle (we assume an average of 2 or 3; this paper), fN_{wct} is the number of tidal maxima per Wilson cycle (we assume an average of 2; this paperwork). PT_{tm} is a representativethe periodtime duration forof each tidal maximum (20 Myr) and PT_{Ept} is the period plate tectonics has been active onage of the Earth (3.34.5 GByr; e.g. Brent 2001). This Fermi estimation suggests that there may have been ~20 super-tidal periods on Earth (N), spanning over 400 Myr (8.9%) of the Earth’s history. This value is corroborated by the results in Table 2.Inputting these assumed values to the equation gives an f_{tot} of 22 and a T_{tot} of 13.3% meaning 440 Myr of Earth history was in tidal maxima. This value is corroborated by the Aurica and Pangea Ultima scenarios (Table 2).

Author contribution

Hannah S. Davies: Conceptualization, Formal Analysis, Investigation, Methodology, Software, Validation, Visualization, Writing – Original draft, Writing – review & editing

J.A. Mattias Green: Conceptualization, Data Curation, Funding Acquisition, Methodology, Project Administration, Resources, Software, Supervision, Validation, Writing – review & editing

Joao C. Duarte: Conceptualization, Funding Acquisition, Project administration, Resources, Supervision, Writing – review & editing.

Acknowledgements

H.S. Davies acknowledges funding from FCT (ref. UID/GEO/50019/2019—Instituto Dom Luiz; FCT PhD grant ref. PD/BD/135068/2017). J.A.M. Green acknowledges funding from NERC (MATCH, NE/S009566/1), an internal travel grant from the School of Ocean Science, and a Santander travel bursary awarded through Bangor University. J.C. Duarte acknowledges an FCT Researcher contract, an exploratory project grant ref. IF/00702/2015, and the FCT project

UID/GEO/50019/2019-IDL. Tidal modelling was carried out using HPCWales and the support of Ade Fewings. We would like to thank Filipe Rosas, Pedro Miranda, Wouter Schellart, and Célia Lee, for insightful discussions and for providing support related to several aspects of the work. We would also like to thank Daniel Pastor-Galán, the anonymous reviewer, and the editor Ira Didenkulova for their efforts in providing constructive comments and moderation which we believe has improved the paper.

The authors declare that they have no conflict of interest.

References

Arbic, B. K. and Garrett, C.: A coupled oscillator model of shelf and ocean tides, Continental Shelf Research, 30, 564–574, https://doi.org/10.1016/j.csr.2009.07.008, 2010.

Bradley, D.C.: Secular trends in the geologic record and the supercontinent cycle, Earth-Sci. Rev., 108, (1–2), 16–33, https://doi.org/10.1016/j.earscirev.2011.05.003, 2011.

Brent, D.G.: The age of the Earth in the twentieth century: a problem (mostly) solved. Geological society special publications. 190(1):205, http://dx.doi.org/10.1144/GSL.SP.2001.190.01.14, 2001.

Burke, K.: Plate Tectonics, the Wilson Cycle, and Mantle Plumes: Geodynamics from the Top, Annu. Rev. Earth Pl. Sci., 39:1-29, doi: 10.1146/annurev-earth-040809-152521, 2011.

~~Byrne, H. M., Green, J. A. M., Balbus, S. A., and Ahlberg, P. E.: Tides: A key driver of the evolution of terrestrial vertebrates?, Proceedings of the National Academy of Sciences of the USA, In review, 2019.~~

~~Carless, J. C., Green, J. A. M., Pelling, H. E., and Wilmes, S. -B: Effects of future sea-level rise on tidal processes on the Patagonian Shelf, Journal of Marine systems, 163, 113-124, https://doi.org/10.1016/j.jmarsys.2016.07.007, 2016~~

Conrad, C. P., and Lithgow-Bertelloni, C.: How Mantle Slabs Drive Plate Tectonics, Science, 298, 207 – 209, doi: 10.1126/science.1074161, 2002.

Davies, H. S, Green, J. A. M, and Duarte, J. C.: Back to the future: Testing different scenarios for the next supercontinent gathering, Global and Planetary Change, 169, 133-144, https://doi.org/10.1016/j.gloplacha.2018.07.015, 2018.

~~Dickey, J. O, et al.: Lunar Laser Ranging: A continuing legacy of the Apollo program, Science, 265, 482 – 490, doi:10.1126/science.265.5171.482, 1994.~~

Duarte, J. C., Schellart, W. P., and Rosas, F. M.: The future of Earth's oceans: consequences of subduction initiation in the Atlantic and implications for supercontinent formation, Geol. Mag., 155 (1), 45–58, https://doi.org/10.1017/S0016756816000716, 2018.

Egbert, G. D., and Erofeeva, S. Y.: Efficient Inverse Modeling of Barotropic Ocean Tides, Journal of Atmospheric and Oceanic Technology, 19, 183 – 204, https://doi.org/10.1175/1520-0426(2002)019%3C0183:EIMOBO%3E2.0.CO;2, 2002.

Egbert, G. D., and Ray, R. D.: Estimates of M2 tidal energy dissipation from Topex/Poseidon altimeter data, Journal of Geophysical Research, 106, 22,475–22,502, https://doi.org/10.1029/2000JC000699, 2001.

Egbert, G. D., Ray, R. D., and Bills, B. G.: Numerical modelling of the global semidiurnal tide in the present day and in the last glacial maximum, Journal of Geophysical Research, 109, C03003, doi: 10.1029/2003JC001973, 2004.

Golonka, J.: Late Triassic and Early Jurassic palaeogeography of the world, Palaeogeogr. palaeocl., 244, 297–307, https://doi.org/10.1016/j.palaeo.2006.06.041, 2007.

~~Green, J. A. M., Green, C. L., Bigg, G. R., Rippeth, T. P., Scourse J. D., and Uehara, K.: Tidal mixing and the Meridional Overturning Circulation from the Last Glacial Maximum, Geophys. res. lett., 36, L15603, doi: 10.1029/2009GL039309, 2009.~~

Green, J. A. M.: Ocean tides and resonance, Ocean Dynam., 60, 1243–1253, doi: 10.1007/s10236-010-0331-1, 2010.

Green, J. A. M., and Huber, M.: Tidal dissipation in the early Eocene and implications for ocean mixing, Geophys. Res. Lett., 40, 2707–2713, https://doi.org/10.1002/grl.50510, 2013.

Green, J. A. M., Huber, M., Waltham, D., Buzan, J., and Wells, M.: Explicitly modelled deep-time tidal dissipation and its implication for Lunar history, Earth Planet. Sci. Lett., 461, 46–53, doi: 10.1002/2017gl076695, 2017.

Green, J. A. M., Molloy, J. L., Davies, H. S., and Duarte, J. C.: Is There a Tectonically Driven Supertidal Cycle? Geophys. Res. Lett., 45, 3568–3576, doi: 10.1002/2017gl076695, 2018.

~~Green, J. A. M., Davies, H. S., Duarte, J. C., Creveling, J. R., and Scotese, C.: Low tides prolonged Snowball Earth, Nat. commun., in review, 2019.~~

~~Harries, P. J., and Little, C. T. S.: The early Toarcian (Early Jurassic) and the Cenomanian–Turonian (Late Cretaceous) mass extinctions: similarities and contrasts, Palaeogeogr. palaeocl., 154, 39 – 66, https://doi.org/10.1016/S0031-0182(99)00086-3, 1999.~~

Hatton, C.J., 1997. The superocean cycle. S. Afr. J. Geol. 100(4), 301-310, 1997.

~~Huber, M., L. Sloan, C. and Shellito, C.: Early Paleogene oceans and climate: A fully coupled modelling approach using NCAR's CSM, in Causes and consequences of globally warm climates in the Early Paleogene, Geol. Soc. America Special Paper, 369, 25–47, Colorado, USA, 2003.~~

Kagan, B.A., and Sundermann, J.: Dissipation of Tidal energy, Paleotides and evolution of the Earth-Moon system, Advances in Geophysics, 38, 1996.

Kagan, B.A.: Earth-Moon tidal evolution: model results and observational evidence, Prog. Oceanog., 40, 109-124, https://doi.org/10.1016/S0079-6611(97)00027-X, 1997.

Killworth, P.: Something stirs in the deep, Nature, 396, 720 – 721, https://doi.org/10.1038/25444, 1998

Kleine, T., Palme, H., Mezger, K., and Halliday, A. N.: Hf-W Chronometry of Lunar Metals and the Age and Early Differentiation of the Moon, Science, 310, 1671 – 1674, doi: 10.1126/science.1118842, 2005.

Miller, E. L., et al.: New insights into Arctic paleogeography and tectonics from U-Pb detrital zircon geochronology, Tectonics, 25, TC3013, doi:10.1029/2005TC001830, 2006.

Mitchell, R. N., Kilian, T. M., Evans, D. A. D.: Supercontinent cycles and the calculation of absolute palaeolongitude in deep time, Nature, 482 (7384), 208–211, https://doi.org/10.1038/nature10800, 2012.

Muller, R. D., et al.: Gplates – Building a Virtual Earth Through Deep time, Geochem. Geophy. Geosy., 19, 7, 2243 – 2261, https://doi.org/10.1029/2018GC007584, 2018.

Munk. W., and Wunsch, C.: Abyssal recipes II: energetics of tidal and wind mixing, Deep Sea Research I, 45, 1977 – 2010, https://doi.org/10.1016/S0967-0637(98)00070-3, 1998.

Murphy, J. B., and Nance, R. D.: Do supercontinents introvert of extrovert?: Sm-Nd isotope evidence, Geol. Soc. Am., 31(10), 873-876, doi: 10.1130/G19668.1, 2003.

Murphy, J. B., and Nance, R. D.: Do Supercontinents turn inside-in or inside-out?, International Geology review, 47:6, 591-619, doi: 10.2747/0020-6814.47.6.591, 2005.

Murphy, J.B., and Nance, R.D.: The Pangea conundrum, Geog. Soc. Of America, 36, 9, 703–706, doi: 10.1130/G24966A.1, 2008.

Nance, D. R., Worsley, T. R., and Moody, J. B.: The Supercontinent Cycle, Scientific American, 259(1), 72 – 78, doi: 10.1038/scientificamerican0788-72, 19898.

Nance, D. R., Murphy, B. J., and Santosh, M.: The supercontinent cycle: A retrospective essay, Gondwana Research, 25(1), 4-29, https://doi.org/10.1016/j.gr.2012.12.026, 2013.

Nield, T.: Supercontinent, Granta Books, London (287 pp.). 2007.

NOAA, ETOPO1 Global relief model. ETOPO1: doi:10.7289/V5C8276M (Accessed on 15/1/18).

Pastor-Galan, D., Nance, D. R., Murphy, B. J., and Spencer, C.J.: Supercontinents: myths, mysteries, and milestones, Geological Soc. London, Special publications, 470, https://doi.org/10.1144/SP470.16, 2018.

Platzmann G. W.: Normal modes of the Atlantic and Indian oceans, Journal of physical oceanography, 5, no 2, 201 – 221, https://doi.org/10.1175/1520-0485(1975)005%3C0201:NMOTAA%3E2.0.CO;2, 1975.

Qin, X., et al.: The GPlates geological information model and markup language, Geosci. Instrum. Methods Data Syst., 1, 111–134, https://doi.org/10.5194/gi-1-111-2012, 2012.

~~Raup, D. M., and Sepkoski, J.J.: Mass Extinctions in the Marine Fossil Record, Science, 215, 4539, 1501 – 1503, doi: 10.1126/science.215.4539.1501, 1982.~~

~~Schmittner, A., and Egbert, G. D.: An improved parameterization of tidal mixing for ocean models, Geosci. Model Dev., 7, 211–224, doi: 10.5194/gmd-7-211-2014, 2014.~~

Scotese, C. R.: Jurassic and cretaceous plate tectonic reconstructions, Palaeogeogr. Palaeocl., 87 (1–4), 493–501, https://doi.org/10.1016/0031-0182(91)90145-H, 1991.

Scotese, C. R.: Palaeomap project. http://www.scotese.com/earth.htm (accessed on 15/1/18), 2003.

~~Signor, P. W.: Biodiversity in Geological time, American Zool, 34, 1, 23 – 32, https://doi.org/10.1093/icb/34.1.23, 1994.~~

Smith, W. H. F., and Sandwell, D. T.: Global seafloor topography from satellite altimetry and ship depth soundings, Science, v. 277, 5334, p. 1956-1962, doi: 10.1126/science.277.5334.1956, 1997.

Stammer, D., et al.: Accuracy assessment of global barotropic ocean tide models, Reviews of Geophysics, 52, 3, https://doi.org/10.1002/2014RG000450, 2014.

~~Stern, R. J., and Gerya, T.: Subduction initiation in nature and models: A review, Tectonophysics, 746, 173 – 198, https://doi.org/10.1016/j.tecto.2017.10.014, 2017.~~

Torsvik, T. H., et al.: Diamonds sampled by plumes from the core-mantle boundary, Nature, 466, 352-357, doi:10.1038/nature09216, 2010.

Torsvik, T. H., et al.: Earth evolution and dynamics – a tribute to Kevin Burke, Canadian Journal of Earth Sciences, 53(11), 1073 – 1087, https://doi.org/10.1139/cjes-2015-0228, 2016.

Wilmes, S. B., and Green, J. A. M.: The evolution of tides and tidal dissipation over the past 21,000 years, J. Geophys. Res. Ocean, 119, https://doi.org/10.1002/2013JC009605, 2014.

~~Wilmes, S. -B., et al.,: Global Tidal Impacts of Large-Scale Ice sheet collapse, J. Geophys. Res-Oceans., 122, 8354 – 8370, https://doi.org/10.1002/2017JC013109, 2017.~~

Wilson, T. J.: 1966, Did the Atlantic Close and then Re-Open?, Nature, 211, 676-681, https://doi.org/10.1038/211676a0, 1966.

Yoshida, M., and Santosh, M.: Future supercontinent assembled in the northern hemisphere, Terra Nova, 23 (5), 333–338, https://doi.org/10.1111/j.1365-3121.2011.01018.x, 2011.

Yoshida, M.: Formation of a future supercontinent through plate motion – driven flow coupled with mantle downwelling flow, Geol. Soc. Am., 44 (9), 755–758, https://doi.org/10.1130/G38025.1, 2016.

Yoshida, M., and Santosh, M.: Geoscience Frontiers voyage of the Indian subcontinent since Pangea breakup and driving force of supercontinent cycles: insights on dynamics from numerical modelling, Geosci. Front., 1–14, https://doi.org/10.1016/j.gsf.2017.09.001, 2017.

Yoshida, M., and Santosh, M.: Voyage of the Indian subcontinent since Pangea breakup and driving force of supercontinent cycles: Insights on dynamics from numerical modelling, Geosci. Front., 9(5), 1279-1292, https://doi.org/10.1016/j.gsf.2017.09.001, 2018.

Zaron, E. D., and Egbert, G. D.: Verification studies for a z-coordinate primitive-equation model: Tidal conversion at a mid-ocean ridge, Ocean Modelling, 14, 3-4, 257–278, https://doi.org/10.1016/j.ocemod.2006.05.007, 2006.

Figure Captions

Figure 1: a) The PD bathymetry in m.

b) as in a but for the degenerate PD bathymetry (see text for details).

c-d) The simulated M2 amplitudes (in m) for the control PD (c) and degenerate PD (d) bathymetries. Note that the colour scale saturates at 2 m.

e-f) as in c-d but showing M2 dissipation rates in Wm^{-2}.

Figure 2: Global M_2 amplitudes for six representative time slices of the Pangea Ultima scenario. The colour scale saturates at 2 m. For the full set of time slices, covering every 20 ~~Ma~~Myr see Supplementary material. Also, note that the figures presented for each scenario display different time slices to highlight periods with interesting tidal signals and that the centre longitude varies between panels to ensure the supercontinent forms in the middle of each figure (where possible).

Figure 3: Normalised (against PD degenerate) globally integrated dissipation rates for the Pangea Ultima (a), Novopangea (b), Aurica (c), and Amasia (d) scenarios. The lines refer to total (solid line), deep (dashed line), and shelf (dot-dashed line) integrated dissipation values. Each super-tidal peak is marked where it reaches its peak, Pac = Pacific, Atl = Atlantic.

Figure 4: As in figure 2 but for the Novopangea scenario.

Figure 5: As in figure 2 but for the Aurica scenario.

Figure 6: As in figure 2 but for the Amasia scenario.

Tables

Table 1: Summary of the number of super-tidal peaks for each scenario.

Supercontinent scenario	Mode of supercontinent formation	Number of super-tidal peaks, incl. PD	Resonant basin(s), including PD	Average normalised (against PD degenerate = 2.2 TW) dissipation
Pangea Ultima	Introversion	5	Atlantic, Pacific, Pacific & Atlantic, Pacific & Atlantic, Pacific	0.877
Novopangea	Extroversion	2	Atlantic, Pacific	0.520
Aurica	Combination	4	Atlantic, Pacific, Atlantic, Pan-Asian	0.647
Amasia	Orthoversion	1	Atlantic	0.723

Table 2: Summary of the total time each scenario was in a super-tidal ~~tidal maximum~~state.

Supercontinent scenario	Number of Supertidal cycles	Timespan~~Full period~~ of supercontinent cycle (from the formation of Pangea to the breakup of the Future Supercontinent) (Myr)	Total ~~period~~ time span of tidal maxima (Myr)	T~~$_{tot}$~~$_{(future)}$ (%)
Pangea Ultima	5	730	100	13.7
Novopangea	2	680	40	5.9
Aurica	4	730	80	11.0
Amasia	1	680	20	2.9

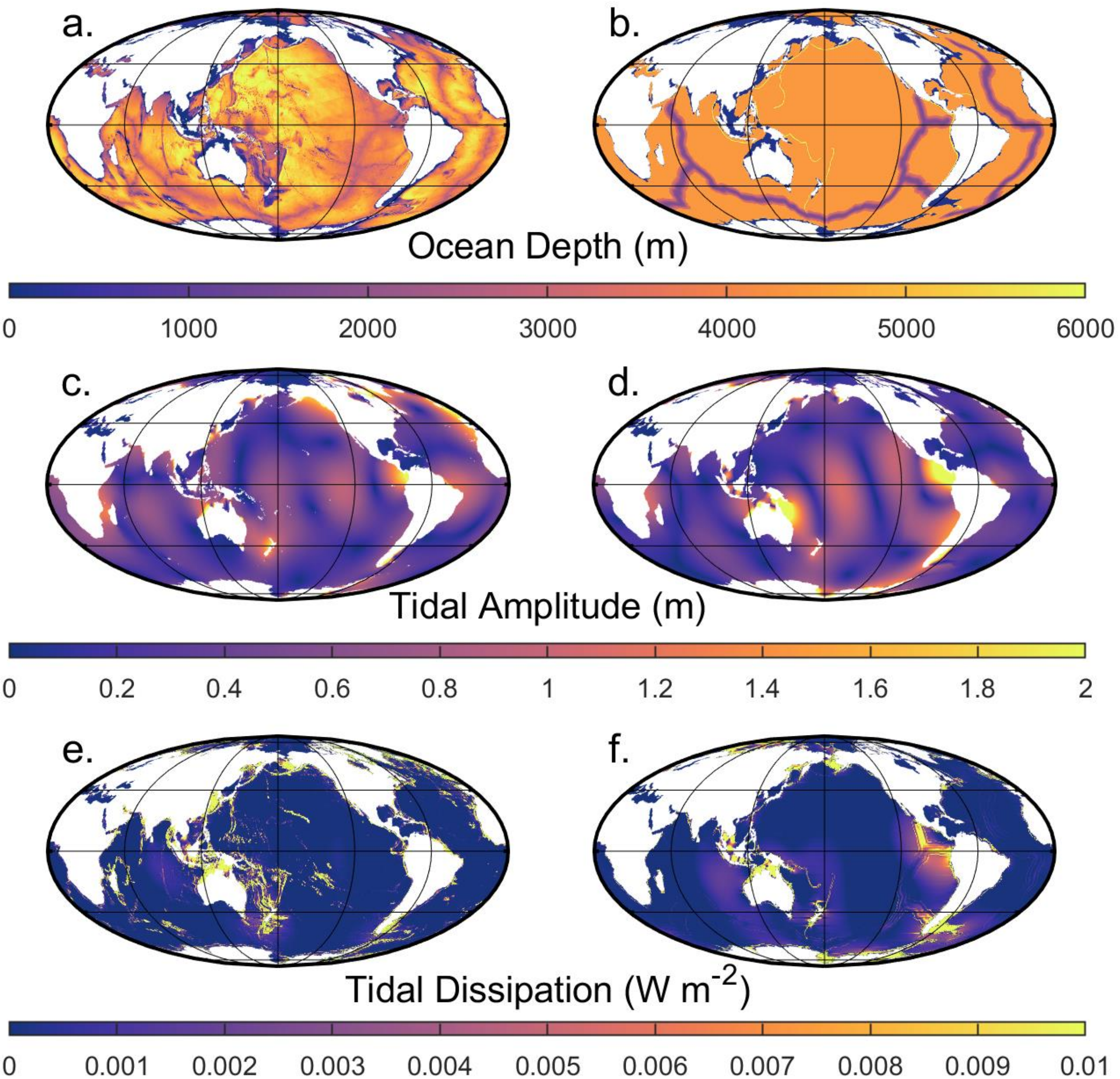
a.
b.
Ocean Depth (m)
0
1000
2000
3000
4000
5000
6000
c.
d.
Tidal Amplitude (m)
0
0.2
0.4
0.6
0.8
1
1.2
1.4
1.6
1.8
2
e.
f.
Tidal Dissipation (W m-2)
0
0.001
0.002
0.003
0.004
0.005
0.006
0.007
0.008
0.009
0.01

Figure 1.

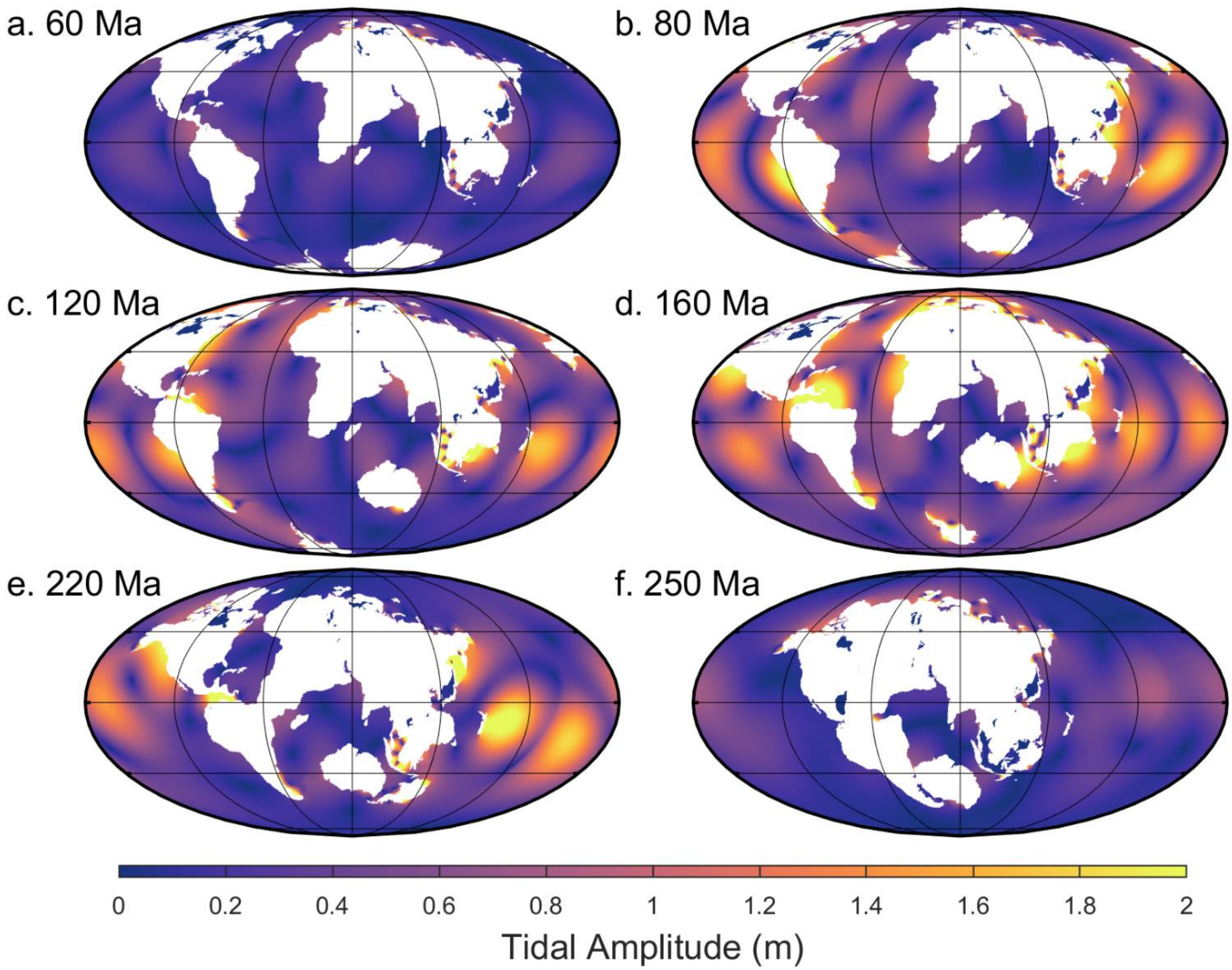
a. 60 Ma
b. 80 Ma
c. 120 Ma
d. 160 Ma
e. 220 Ma
f. 250 Ma
0
0.2
0.4
0.6
0.8
1
1.2
1.4
1.6
1.8
2
Tidal Amplitude (m)

Figure 2.

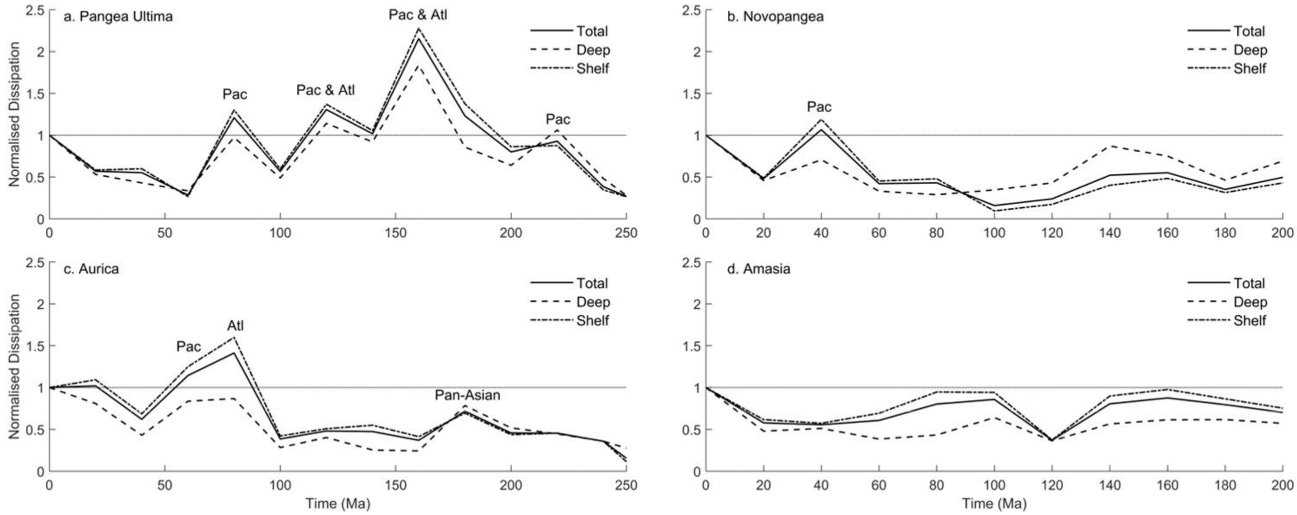
a. Pangea Ultima
b. Novopangea
c. Aurica
d. Amasia
Total
Deep
Shelf
Pac
Pac & Atl
Atl
Pan-Asian
Normalised Dissipation
Time (Ma)
0
0.5
1
1.5
2
2.5
50
100
150
200
250
20
40
60
80
120
140
160
180

Figure 3.

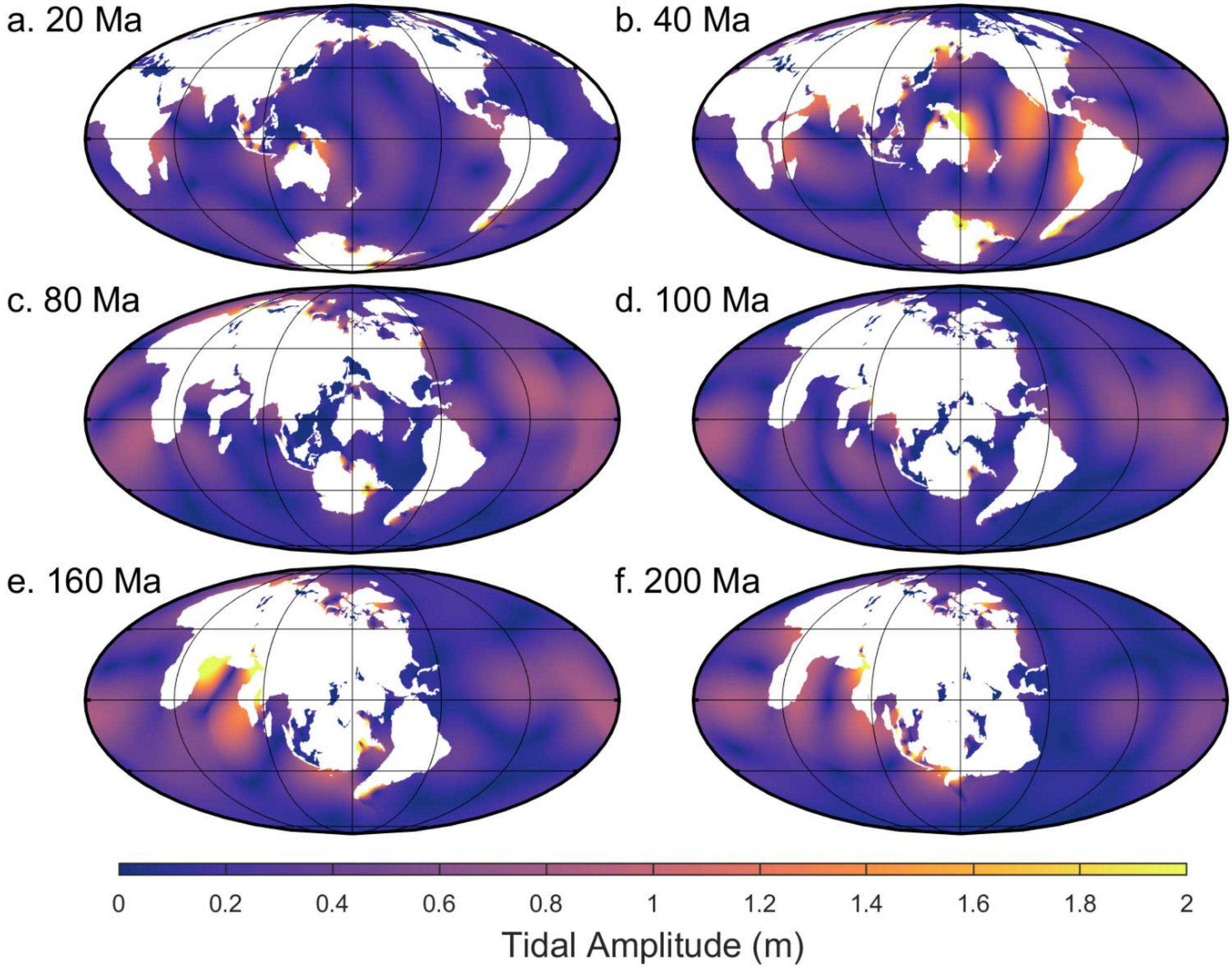

a. 20 Ma
b. 40 Ma
c. 80 Ma
d. 100 Ma
e. 160 Ma
f. 200 Ma
0
0.2
0.4
0.6
0.8
1
1.2
1.4
1.6
1.8
2
Tidal Amplitude (m)

Figure 4.

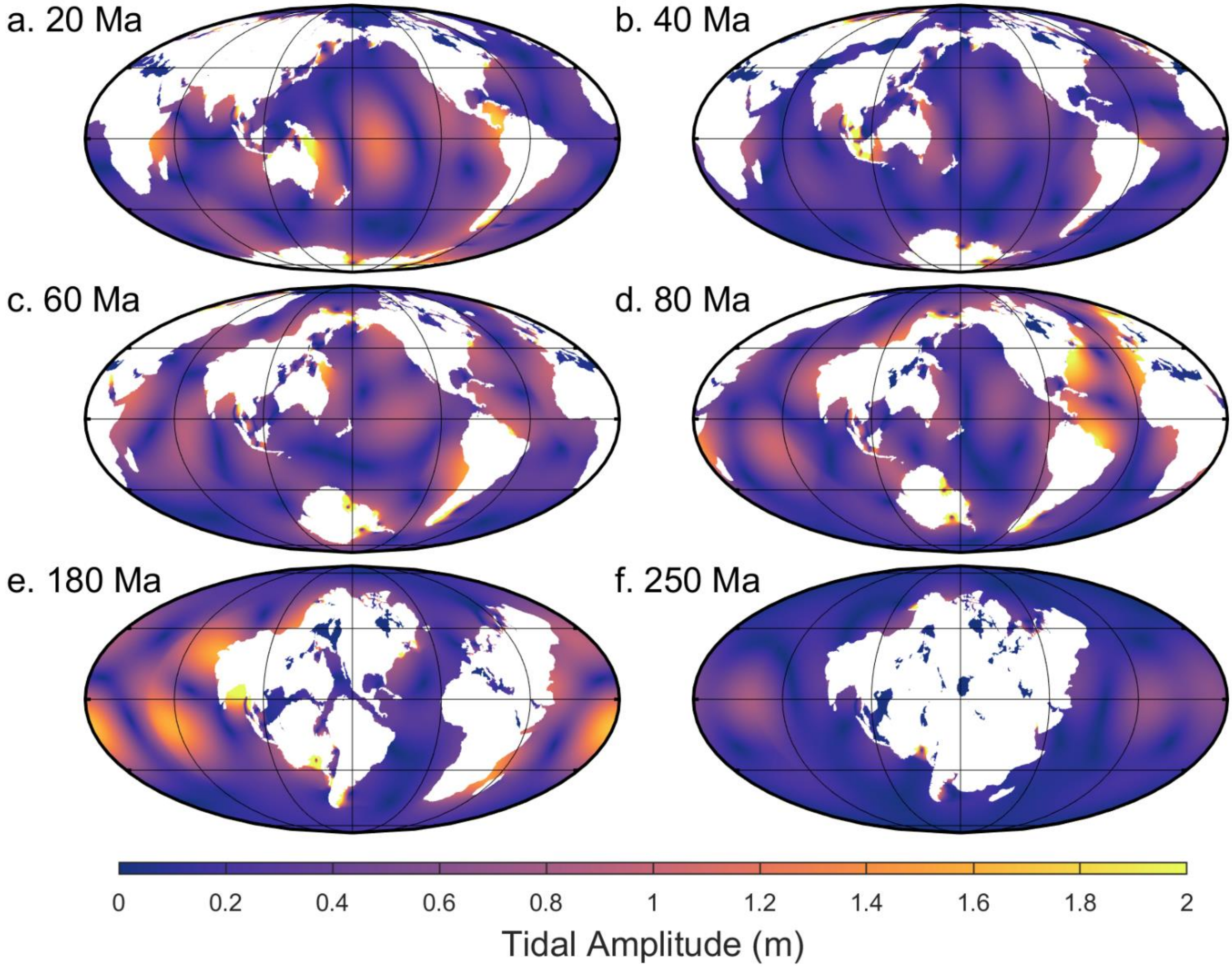
a. 20 Ma
b. 40 Ma
c. 60 Ma
d. 80 Ma
e. 180 Ma
f. 250 Ma
0
0.2
0.4
0.6
0.8
1
1.2
1.4
1.6
1.8
2
Tidal Amplitude (m)

Figure 5.

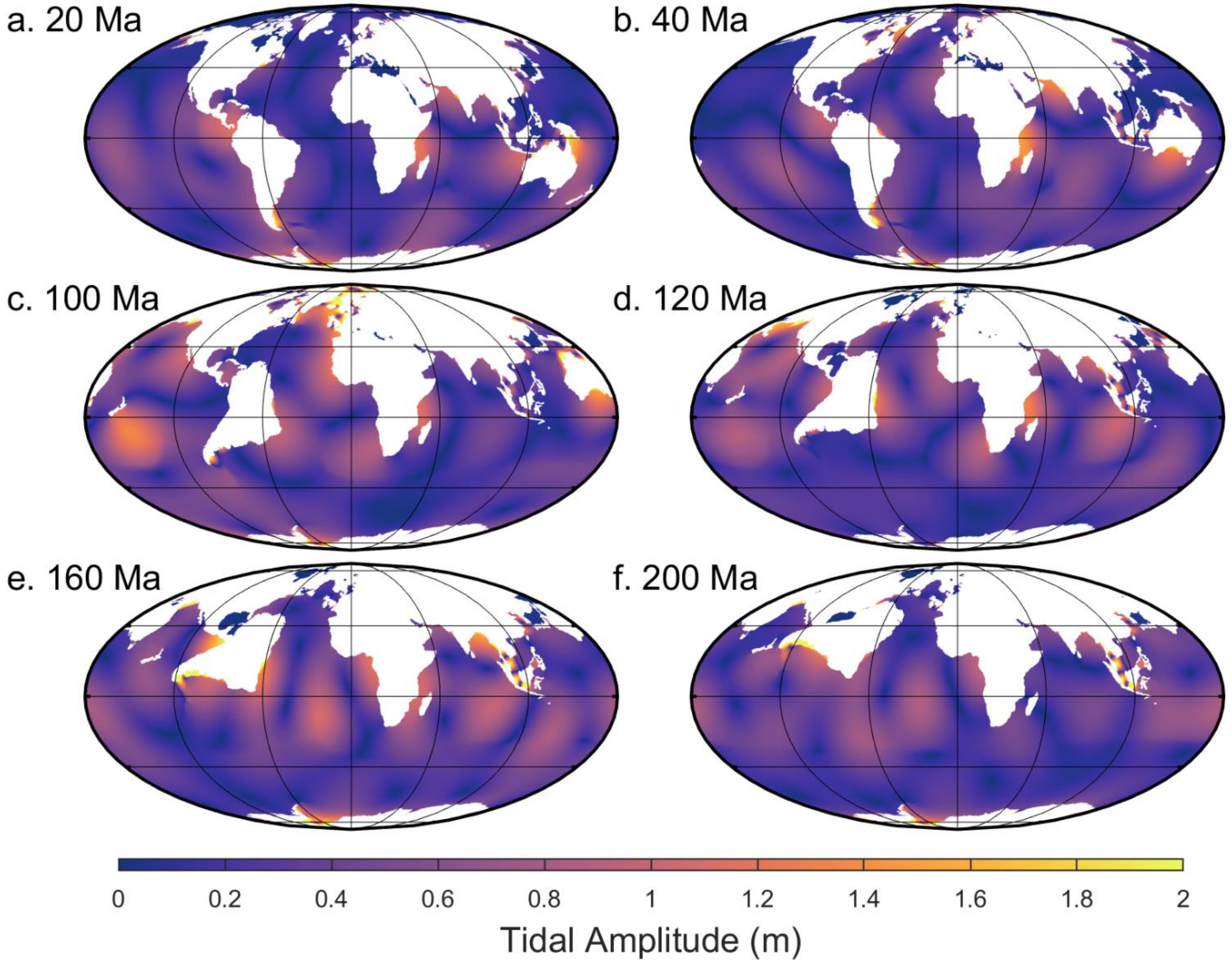
a. 20 Ma
b. 40 Ma
c. 100 Ma
d. 120 Ma
e. 160 Ma
f. 200 Ma
0
0.2
0.4
0.6
0.8
1
1.2
1.4
1.6
1.8
2
Tidal Amplitude (m)

535

Figure 6.